

Dynamic response of underground box structure subjected to explosion seismic wave

Houxu Huang^{*1}, Jie Li¹, Xiaoli Rong¹, Pengxian Fan¹ and Shufang Feng²

¹State Key Laboratory of Disaster prevention and Mitigation of Explosion and Impact,
PLA University of Science and Technology, Nanjing, China

²Institute of Engineering Research and Design, Headquarters of Shenyang Military Area, Shenyang, China

(Received September 15, 2015, Revised November 28, 2015, Accepted December 2, 2015)

Abstract. In this paper, the underground box structure is discretized as a system with limited freedoms, and the explosion seismic wave is regarded as series of dynamic force acting on the lumped masses. Based on the local deformation theory, the elastic resistances of the soil are simplified as the effects of numbers of elastic chain-poles. Matrix force method is adopted to analyze the deformation of the structure in elastic half space. The structural dynamic equations are established and by solving these equations, the axial force, the moment and the displacement of the structure are all obtained. The influences of size ratio, the incident angle and the rock type on the dynamic response of the underground box structure are all investigated through a case study by using the proposed method.

Keywords: explosion seismic wave; underground box structure; dynamic response; matrix force method

1. Introduction

The dynamic response of the underground structure under the action of the explosion seismic wave is directly related to the safety of the underground defense project. Thus, the study of the dynamic response of the underground structure is of great importance and to develop an appropriate algorithm to study the soil-structure interaction seems necessary and meaningful. The study of the soil-structure interaction developed fast since the 1970s, R.Nateghi *et al.* (2009) studied the effect of the blast vibration on the tunnel lining through the field monitoring. T.Akiyoloi and K.Fuschida (1984) obtained the solution of the wave equations by using the Bessel function and used them to study the longitudinal wave's effect on the tunnel lining. J.Penzen *et al.* (1988) simulated the dynamic response of the underground structure under the action of the internal explosion, and obtained the dynamic response equation by using the simplified elastic support lining. Ma (2008) studied the dynamic response of the concrete lining by using the small normal weight of explosion. Shen *et al.* (2007) developed a soil anti-explosion device and studied the damage effects of the explosion seismic wave on the underground structure by using the indoor experiments. Xin *et al.* (2009) studied the dynamic response of different underground structures

*Corresponding author, Doctoral Candidate, E-mail:wuhanhp14315@163.com

by using the cylindrical explosion simulation device. Gao *et al.* (2010) studied the effects of the Poisson's ratio, the shear modulus and the thickness of the lining on the dynamic response of the lining, which is under the effects of a sudden applied loading. Mazek and Wahab (2015) studied the impact of the composite materials on the underground structures that performance against the blast wave. Gu (2015) gave the practical considerations in designing the underground station structures for seismic wave. Besides, with the fast development of the computer, the numerical method is also widely used in the analysis of the underground structure under the action of explosion (Feldgun *et al.* 2008, Guo *et al.* 2004, Lu *et al.* 2005, Shin *et al.* 2011).

Based on the above analyses, we can find that the study of the dynamic response of the structure to the action of explosion is mainly based on test (including the indoor experiments and field tests) and numerical analysis. Although we can obtain much useful information from a successful test, the explosion test, in so many situations, is difficult, dangerous and what's more, too much expensive. Thus, the numerical analysis, which is cheaper and repeatable, seems to be a good choice for studying this kind of problem. The numerical analysis is mostly based on the business software, such as LS-DYNA, AUTODYN and FLAC, but the newly developed numerical analysis method is rare and to some extent, should be encouraged.

In this paper, based on the lumped mass method, the underground structure is discretized as a system with limited freedoms, and the seismic wave is regarded as series of dynamic force acting on the structure. The dynamic response of the underground structure under the action of the explosion seismic wave is calculated by using the matrix force method and the corresponding dynamic response equations are established. The proposed method can simulate the effects of different types of shock waves on the underground structure. Compared with the response spectrum method and the wave theory approaches, the theory of our method is simpler, and the adaptability of our method to different wave loadings is better.

2. The matrix force method

Assuming that the underground box structure is closed, replacing the unknown force with chain-pole and representing the loading acting on the structure as $\{p\}$.

The sizes of the underground structure and the shock wave acting on the structure are shown in

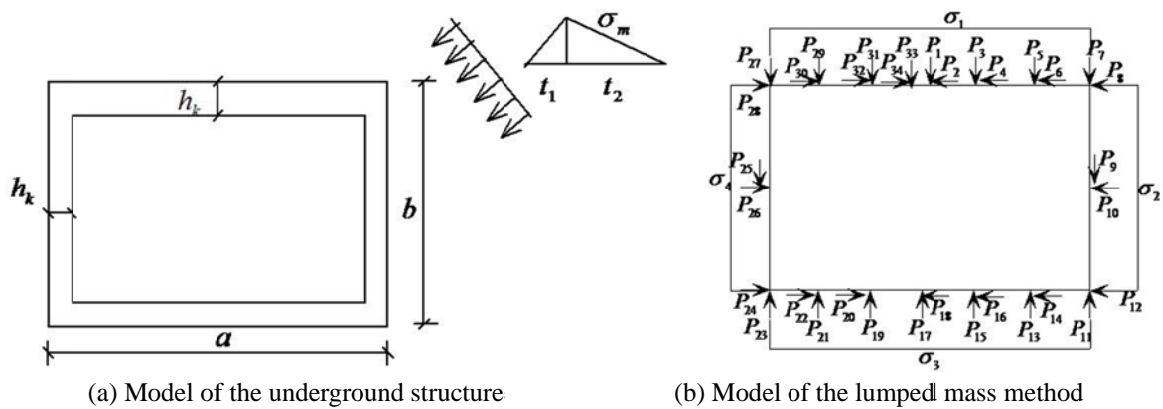


Fig. 1 The model of the underground box structure

Fig. 1(a), the structure is simplified as the composition of numbers lumped masses with limited freedoms, which is shown in Fig. 1(b). According to the compatibility of deformation, the equations for the matrix force method of the whole structure is

$$[F_{xx}][X] + [F_{xp}][p] = 0 \tag{1}$$

the internal force matrix $[S]$, which represents the internal force caused by the external force and the unknown force on the studied points, can be expressed as

$$[S] = [r_{sp}][p] + [\bar{r}_{sx}][X] \tag{2}$$

$[F_{xx}]$ and $[F_{xp}]$ are the flexibility matrixes of unit force and unit external force

$$[F_{xx}] = [\bar{r}_{sx}]^T [F_0] [\bar{r}_{sx}], \quad [F_{xp}] = [\bar{r}_{sx}]^T [F_0] [r_{sp}] \tag{3}$$

where $[F_0]$ is the flexibility matrix of the whole structure, $[r_{sp}]$ is the variant matrix of unit internal force that is caused by the unit external force, $[\bar{r}_{sx}]$ is the variant matrix of unit internal force that is caused by the unit unknown force.

3. Dynamic equations of the structure

The forced vibration of the structure that can take the systems' flexibility into consideration can be expressed as the following non-homogeneous differential equation system

$$y + FM\ddot{y} + FC\dot{y} = Fp \tag{4}$$

where $p = \{p_i\}_{34}$ is the column vectors of the dynamic force, $M = [m_{ij}]_{34}$ is the diagonal matrix of the lumped mass, $F = [f_{ij}]_{34 \times 34}$ is the unit displacement matrix of the lumped mass, $C = [C_{ij}]_{34}$ is the damping matrix, $y = \{y_i\}_{34}$, $\dot{y} = \{\dot{y}_i\}_{34}$, $\ddot{y} = \{\ddot{y}_i\}_{34}$ are respectively the vectors of the displacement, velocity and acceleration of the lumped mass.

3.1 The load, mass and damping matrixes

The column vector p of the dynamic force can be expressed as the sum of the column vector of every wave k , i.e.

$$p = \sum_{k=1}^n p^k \tag{5}$$

where n represents the number of the waves that is simultaneously taken into consideration, and the element of $p^k = \{p_i^k\}_{34}$ can be expressed as

$$p_i^k = S_i^k F_i^k \quad (i=1,2,\dots,34) \tag{6}$$

$S^k = [S_i^k]_{34}$ is the maximum value of the concentrated dynamic force under the situation that the k -th wave acting on the lumped masses; the elements in $F^k = \{F_i^k\}_{34}$ represent the variant of the

dynamic force, which is caused by the k -th wave, with time, and it is can be expressed as the following form

$$F_i^k = \left[\frac{t - t_{0i}^k}{\tau_{1i}^k} \delta(\tau_{1i}^k - t_{0i}^k - t) + \frac{\tau_{2i}^k + t_{0i}^k - t}{\tau_{2i}^k - \tau_{1i}^k} \delta(t - \tau_{1i}^k - t_{0i}^k) \right] \cdot \delta(t - t_{0i}^k) \cdot t_{0i}^k (\tau_{2i}^k - t_{0i}^k - t) \quad (7)$$

where t_{0i}^k , τ_{1i}^k and τ_{2i}^k are respectively the arrival time, the increase time and the duration of the k -th wave on the i -th point, and $\delta(t)$ has the following form

$$\delta(t) = \begin{cases} 0 & (t > 0) \\ 1 & (t \leq 0) \end{cases} \quad (8)$$

$\sigma_1, \sigma_2, \sigma_3, \sigma_4$ in Fig. 1(b), represent the maximum pressures of the waves on the studied points, and the distribution of the pressure acting on the structure can be expressed as

$$\sigma_i^k = \sigma_m^k \left[k_0 \cos^2(\alpha^k - \varphi_i) + \frac{\nu}{1 - \nu} \sin^2(\alpha^k - \varphi_i) \right] \quad (9)$$

where σ_m^k and α^k are respectively the maximum pressure and angle corresponding to the arrival of the k -th wave at the structure, ν is the Poisson's ratio, k_0 is the reflection coefficient and has the following form

$$k_0 = \frac{2}{1 + C_s \rho_s / (C_k \rho_k)} \quad (10)$$

where C_s and C_k are respectively the velocity of the wave in the soil and structure, ρ_s and ρ_k are respectively the density of the soil and the structure.

The included angles between the normal axis of the structure and the normals of each section are

$$\varphi_i = \begin{cases} 0 & i = 1 \\ \pi/2 & i = 2 \\ \pi & i = 3 \\ 3\pi/2 & i = 4 \end{cases} \quad (11)$$

the lumped mass matrix of the system is

$$\mathbf{M} = \begin{bmatrix} m_{11} & & & 0 \\ & m_{22} & & \\ & & \ddots & \\ 0 & & & m_{34,34} \end{bmatrix}_{34 \times 34} \quad (12)$$

where $m_{ii}(i=1,2,\dots,34)$ are the masses of the studied points and can be expressed by the piecewise function

$$m_{ii} = \begin{cases} \frac{1}{12}\rho_k ah_k + \frac{1}{36}\rho_s ah_s & i = 1,2,33,34 \\ \frac{1}{6}\rho_k ah_k + \frac{1}{18}\rho_s ah_s & i = 3,\dots,6,13,\dots,22,29,\dots,32 \\ \left(\frac{1}{12}a + \frac{1}{4}b\right)\rho_k h_k + \left(\frac{1}{36}a + \frac{1}{12}b\right)\rho_s h_s & i = 7,8,11,12,23,24,27,28 \\ \frac{1}{2}\rho_k bh_k + \frac{1}{6}\rho_s bh_s & i = 9,10,25,26 \end{cases} \quad (13)$$

where h_k and h_s are respectively the thicknesses of the structure and the vibration medium around the structure, a, b are the lengths of the structure, as shown in Fig. 1(a).

When calculating the dynamic response of the structure, the viscous friction model is adopted and the damping matrix of the system can be expressed as

$$C = \alpha_0 M + \alpha_1 K \quad (14)$$

where α_0 and α_1 are the coefficients, K is the stiffness matrix.

3.2 The unit displacement matrix

In order to study the interaction of the soil and the structure, the Chain-pole method is adopted. The structure is simplified as that shown in the following Fig. 2(a), and in Fig. 2(b), the middle of the baseplate is fixed, while the middle of the roof is cut and two new sections, which is under the action of moment X_1 and axial force X_2 , are exposed. The regular equation of the structure can be expressed as the following form

$$BX = D \quad (15)$$

where X represents the matrix of the unknowns, $B = [\delta_{ij}]$ is the factor matrix.

When considering the deformations of the structure and rock, under the action of internal force (including the moment, the axial force and the shear force), the following equations are obtained

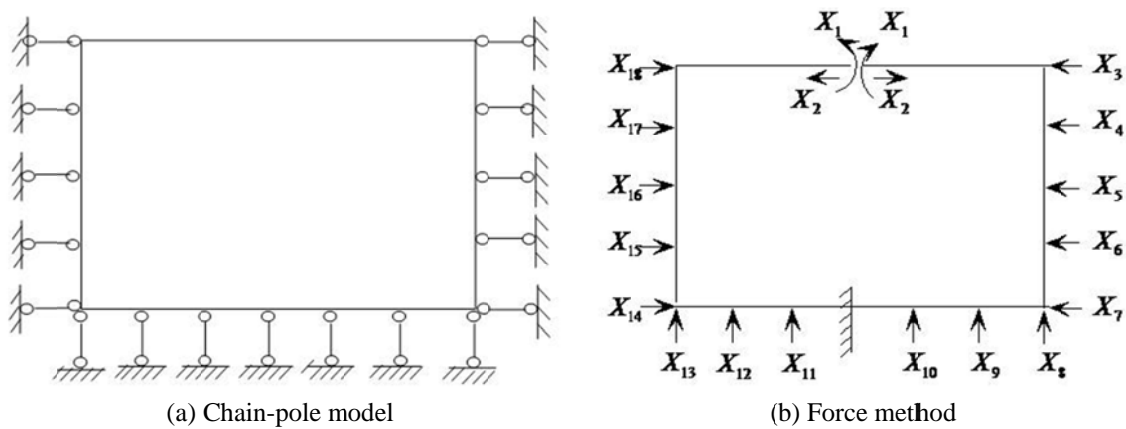


Fig. 2 The schematic diagram of Chain-pole Method

$$\begin{cases} \delta_{ij} = U_{ij} + y_{2,ij} \\ U_{ij} = \sum \int \frac{M_i M_j}{E_k J} ds + \sum \frac{N_i N_j}{E_k A} ds + \sum \frac{\gamma Q_i Q_j}{G_k A} ds \\ y_{2,ij} = \begin{cases} 0 & (i \neq j) \\ 1/kbl_i & (i = j) \end{cases} \end{cases} \quad (16)$$

Where E_k and G_k are respectively the elastic modulus and shear modulus of the structure, J is the inertia of the studied cross section, A is the section area, k is the coefficient of the elastic foundation, γ is the correction factor, l_i is the length of the calculated part and can be expressed as

$$l_i = \begin{cases} a/6 & i = 1 \dots 3, 10 \dots 15, 22 \dots 24 \\ b/4 & i = 5 \dots 8, 17 \dots 20 \\ 0 & i = 4, 9, 16, 21 \end{cases} \quad (17)$$

taking the effect of the elastic foundation into consideration and its deformation is

$$y_{3,ij} = \begin{cases} 0 & (i \neq j) \\ h_2(1 - 2\nu_2^2)/E_2 bl_i & (i = j) \end{cases} \quad (18)$$

where h_2 , ν_2 and E_2 are respectively the thickness, the Poisson's ratio and the elastic modulus of the elastic foundation, thus, the expressions of matrixes \mathbf{B} and \mathbf{D} can be expressed as

$$\mathbf{B} = \mathbf{L}_M^T \mathbf{B}_M \mathbf{L}_M + \mathbf{L}_N^T \mathbf{B}_N \mathbf{L}_N + \mathbf{L}_Q^T \mathbf{B}_Q \mathbf{L}_Q + \mathbf{F}_1, \quad \mathbf{D} = \mathbf{L}_M^T \mathbf{B}_M \mathbf{L}_{MP} + \mathbf{L}_N^T \mathbf{B}_N \mathbf{L}_{NP} + \mathbf{L}_Q^T \mathbf{B}_Q \mathbf{L}_{QP} + \mathbf{F}_P \quad (19)$$

where \mathbf{L}_M , \mathbf{L}_N and \mathbf{L}_Q are the matrixes of the moment, the axial force and the shear force, which are generated under the action of unit unknown force, \mathbf{L}_M^T , \mathbf{L}_N^T and \mathbf{L}_Q^T are the corresponding transposed matrixes; \mathbf{L}_{MP} , \mathbf{L}_{NP} and \mathbf{L}_{QP} are the matrixes of the moment, the axial force and the shear force under the action of unit dynamic force, \mathbf{L}_{MP}^T , \mathbf{L}_{NP}^T and \mathbf{L}_{QP}^T are the corresponding transposed matrixes; \mathbf{B}_M , \mathbf{B}_N and \mathbf{B}_Q are the flexibility matrixes; \mathbf{F}_1 represents the resistance of the elastic foundation to the base of the structure; \mathbf{F}_P represents the build-in effect between the elastic foundation and the middle of the baseplate. Considering that the expressions of the matrixes in Eq. (19) are complex, therefore, we won't give their detailed expressions here.

By solving Eq. (15), the unknown force matrixes are obtained

$$\bar{\mathbf{M}} = \mathbf{L}_M \mathbf{X} + \mathbf{L}_{MP}, \quad \bar{\mathbf{N}} = \mathbf{L}_N \mathbf{X} + \mathbf{L}_{NP}, \quad \bar{\mathbf{Q}} = \mathbf{L}_Q \mathbf{X} + \mathbf{L}_{NP} \quad (20)$$

the displacement matrix in Eq. (4) can be expressed as

$$\mathbf{A} = \mathbf{L}_{MP}^T \mathbf{B}_M \bar{\mathbf{M}} + \mathbf{L}_{NP}^T \mathbf{B}_N \bar{\mathbf{N}} + \mathbf{L}_{QP}^T \mathbf{B}_Q \bar{\mathbf{Q}} + \bar{\mathbf{A}} \quad (21)$$

matrix $\bar{\mathbf{A}}$ is added to consider the possible displacement of the middle of the baseplate, as shown in Fig. 2(b), the elements in $\bar{\mathbf{A}}$ can be expressed as

$$\bar{\mathbf{A}} = \mathbf{d}^T \mathbf{a} \quad (22)$$

where \mathbf{d} represents the elements in the last three rows of matrix \mathbf{D} , \mathbf{a} represents the elements in the last three rows of matrix \mathbf{X} .

4. Application

The parameters for the underground box structure are as follows, the thicknesses of the roof, baseplate and the side wall are respectively 0.8 m, 0.6 m and 0.6 m. The sizes of the outer and internal contours are 3.6 m×5.2 m and 2.2 m×4.0 m, respectively. The parameters of the medium around the reinforced concrete structure are shown in the following Table 1.

4.1 Size ratio's effect on the dynamic response

The size ratio is represented as $s=a/b$, and when $\theta=90^\circ$, the incident direction of the wave is in the vertical direction, in this situation, the dynamic responses of the structure corresponding to $s=1, 1.5, 2.0$ are as follows.

As shown in Fig. 3, the size ratio has a directly influence on the structure's dynamic response, when $\theta=90^\circ$, with the increasing of s , the horizontal displacement of the side wall will decrease while the vertical displacement of the roof will increase.

As shown in Figs. 4(a) and 5(a), the larger the value of s , the smaller the maximum values of the moment and axial force of the side wall, but as shown in Figs. 4(b) and 5(b), the size ratio seems to has no obvious effect on the maximum values of the moment and axial force of the roof.

4.2 The incident angle's effect on the dynamic response

The incident angles adopted here are $\theta=0^\circ, 30^\circ, 45^\circ, 60^\circ, 90^\circ$ and the dynamic responses are as follows.

Table 1 Physical parameters used in the analysis

Medium	density ρ (kg/m ³)	Elastic modulus E (GPa)	Poison's ratio ν
Reinforced concrete	2500	37.8	0.2
soil	1950	0.07	0.42

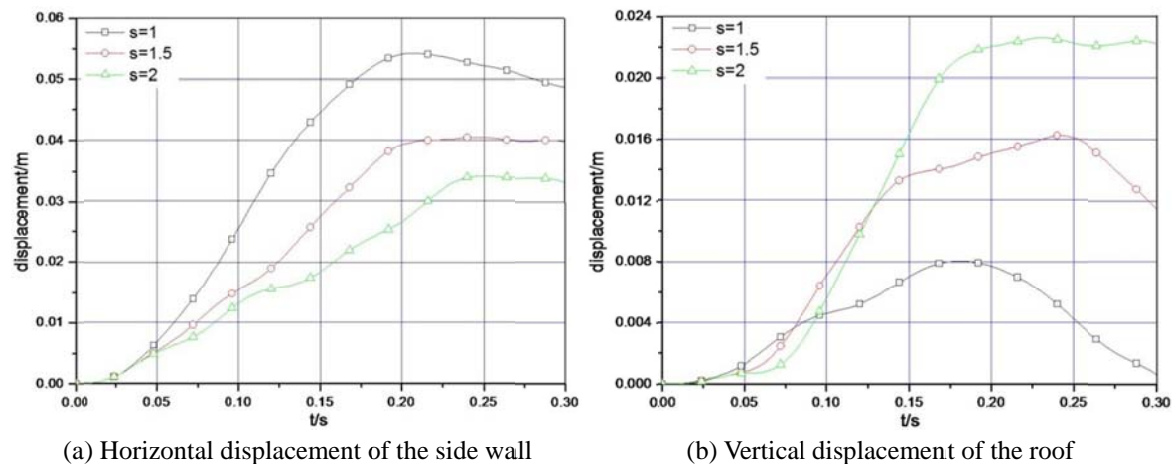
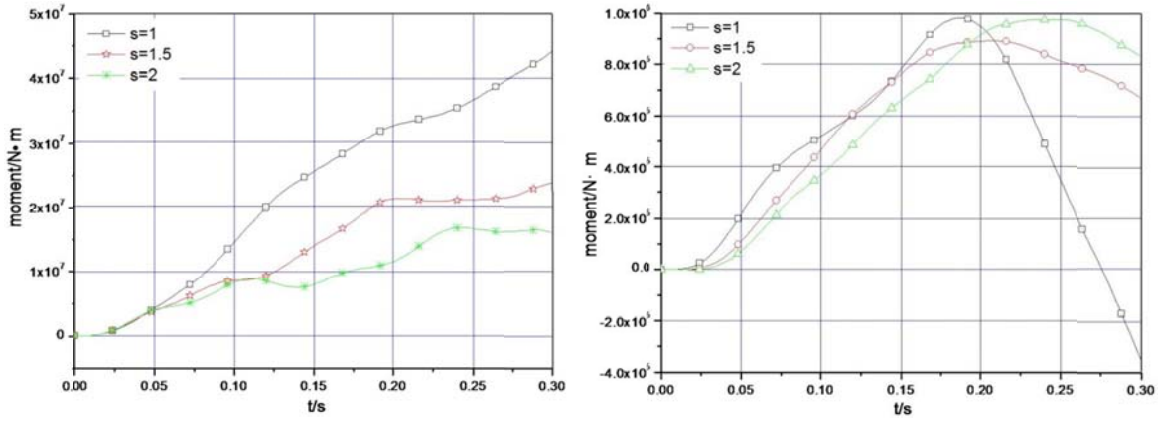
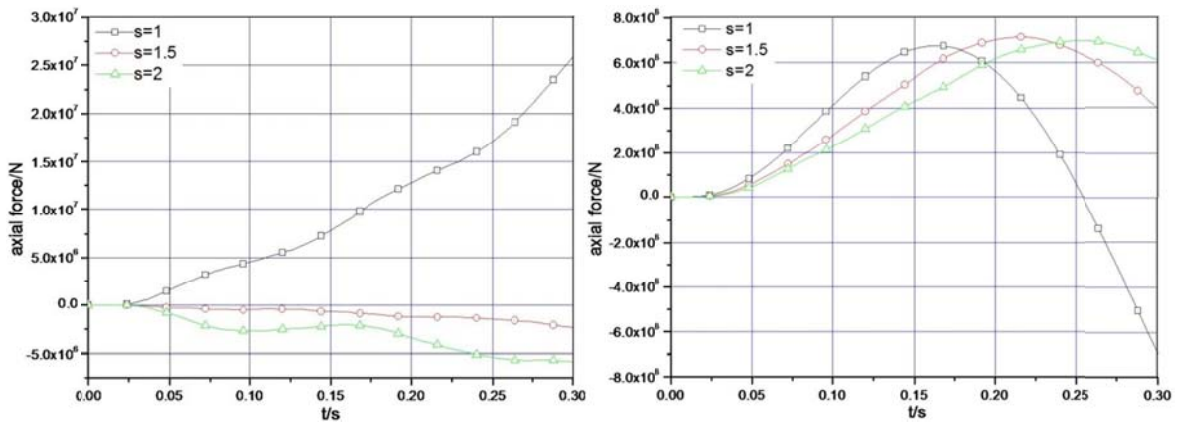


Fig. 3 Time-history curves of the displacement



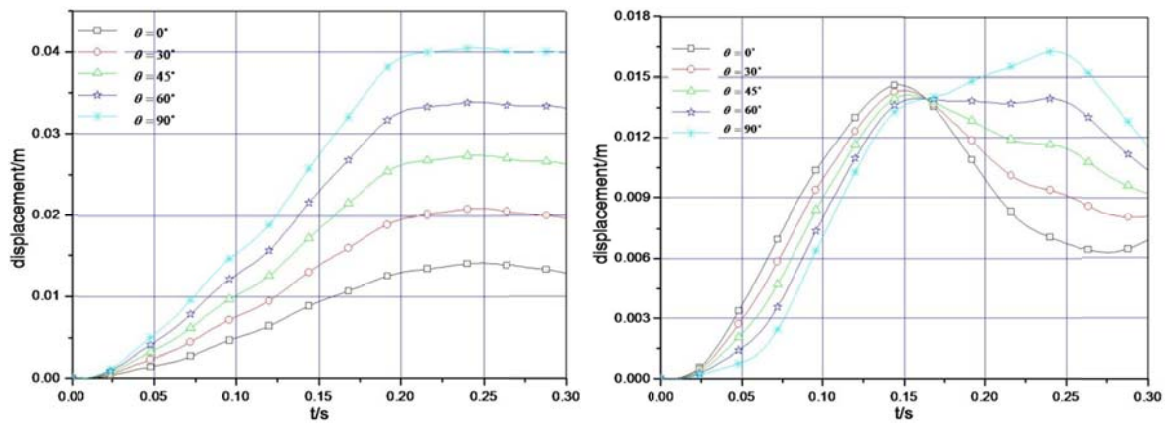
(a) Moment of the side wall (b) Moment of the roof

Fig. 4 Time-history curves of the moment



(a) Axial force of the side wall (b) Axial force of the roof

Fig. 5 Time-history curves of the axial force



(a) Horizontal displacement of the side wall (b) Vertical displacement of the roof

Fig. 6 Time-history curves of the displacement

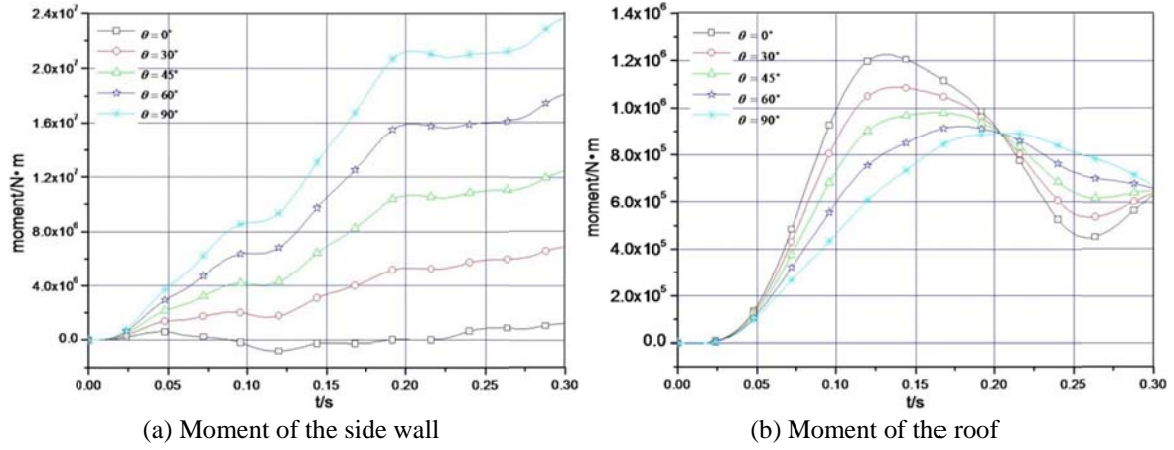


Fig. 7 Time-history curves of the moment

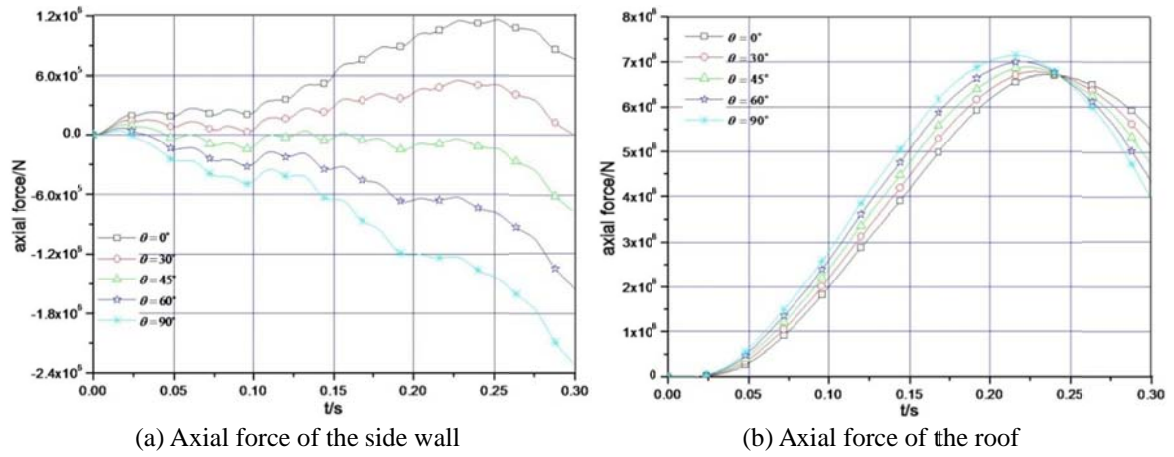


Fig. 8 Time-history curves of the axial force

As shown in Figs. 6(a) and 7(a), the larger the incident angle, the larger the horizontal displacement and moment of the side wall, but as shown in Figs. 6(b) and 7(b), with the increasing of the incident angle, the vertical displacement and moment of the roof will first decrease and then increase. In Fig. 6(b), the vertical displacement will decrease when $t \leq 0.17s$ and increase when $t > 0.17s$, but in Fig. 7(b), the time to separate the decrease and increase phases is $t = 0.20s$.

As shown in Fig. 8(a), with the increasing of the incident angle, the axial force of the side wall will change from pressure to tension, and the axial force of the side wall reaches its minimum value when $\theta = 45^\circ$. The variant of the axial force of the roof, which is shown in Fig. 8(b), is similar with that of the vertical displacement and moment shown in Figs. 6(b) and 7(b), but the difference is that, with the increasing of the incident angle, the axial force of the roof will increase when $t \leq 0.24s$, and decrease when $t > 0.24s$, i.e., first increase and then decrease.

4.3 The rock type's effect on the dynamic response

In order to investigate the rock type's effect on the dynamic response, five kinds of rock are chosen and the corresponding physical parameters are shown in the following Table 2 and the incident angle is $\theta = 90^\circ$.

As shown in Fig. 9, with the decreasing of the rock rigidity, both the horizontal displacement of the side wall and the vertical displacement of the roof will increase obviously.

Table 2 Physical parameters of the rock

Rock	Density ρ (kg/m ³)	Elastic modulus E (GPa)	Poisson's ratio ν
1	2700	33	0.15
2	2600	20	0.22
3	2400	10	0.26
4	2200	3	0.32
5	2000	1.3	0.33

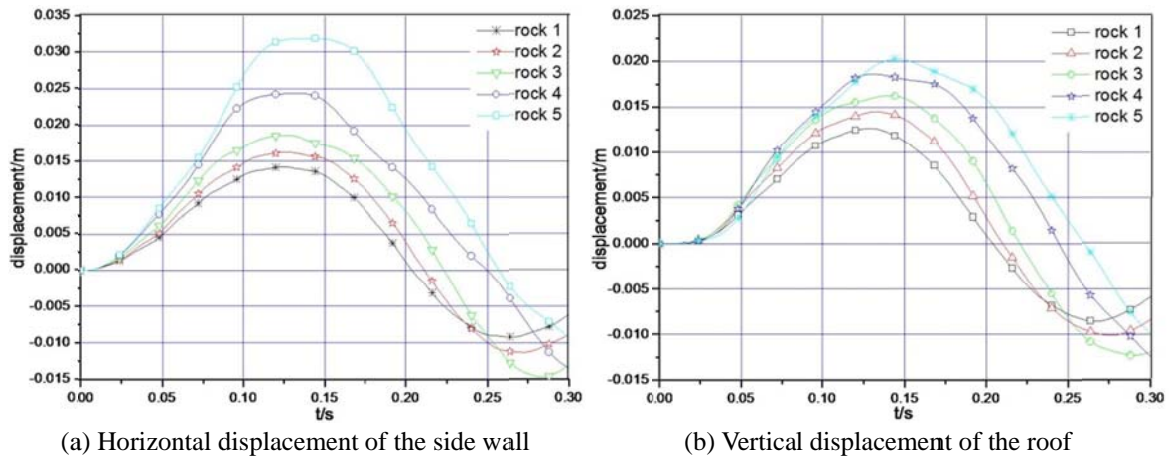


Fig. 9 Time-history curves of displacement

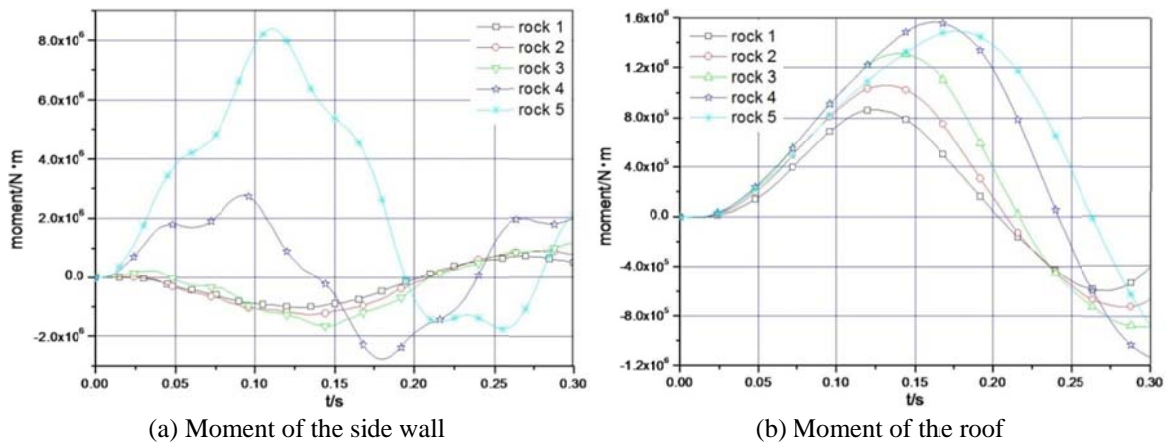


Fig. 10 Time-history curves of the moment

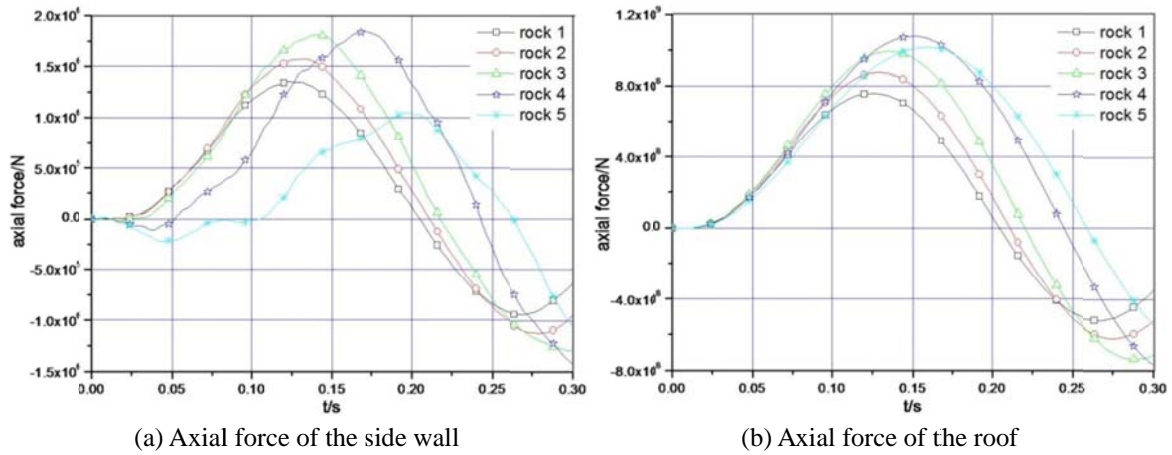


Fig. 11 Time-history curves of the axial force

As shown in Fig. 10(a), as the rigidity of the rock decreasing, the moment of the side wall will increase sharply. But as shown in Fig. 10(b), although the moment of the roof will increase with the decreasing of the rigidity of the rock, compared with the effect of the rock rigidity on the moment of the side wall, the rock rigidity's effect on the moment of the roof is not so obvious.

As shown in Fig. 11, with the decreasing of the rock rigidity, both the axial force of the side wall and the roof will increase obviously, but the curve of rock 5 in both Figs. 11(a) and 11(b) also show that the axial force will decrease if the rock rigidity is too low, which means, it is possible to relieve the axial force concentration by adding an elastic layer of lower impedance to the interval of the rock and structure.

5. Conclusions

In this paper, based on the matrix force method, a new method is proposed, the dynamic response of the underground box structure subjected to the explosion seismic wave is analyzed with the new method and the following conclusions are obtained.

- Both the size ratio s and the incident angle θ have obvious effects on the dynamic response of the underground box structure. Generally speaking, the displacement, the moment and the axial force will reach their maximum values, under the situation either the size ratio $s = 1$ or the incident angle $\theta = 90^\circ$.
- The rigidity of the rock has a significant effect on the dynamic response. Both the displacement and the moment of the structure will increase with the decreasing of the rock rigidity, the axial force concentration corresponding to the rock of lower rigidity will be smaller, and it is possible to relieve the axial force concentration by using elastic layer of lower impedance.

Acknowledgements

The authors would like to express their sincere gratitude to the financial support by the

National Key Basic Research Program of China (Grant No.2013CB036005) and National Natural Science Foundation of China (Grant No.51527810, 51309233), in addition, their appreciation also goes to the editor and the anonymous reviewers for their valuable comments.

References

- Abdelnaby, A.E. and Elnashai, A.S. (2015), "Numerical modeling and analysis of RC frames subjected to multiple earthquakes", *Earthq. Struct.*, **9**(5), 957-981.
- Akiyoloi, T. and Fushida, K. (1984), "Soil-pipelines interaction through a frictional interface during earthquake", *Soil Dyn. Earthq. Eng.*, **3**(1), 77-81.
- Bulson, P.S. (1997), *Explosive loading of engineering structures*, Spon Press, London, UK.
- Drake, J.L., Walker, R.E. and Slawson, T. (1989), "Backfill effect on buried structure response", *Proceeding of the Fourth International Symposium on the interaction of Non-nuclear Munitions with Structure*.
- Feldgun, V.R., Kochetkov, A.V. and Karinski, Y.S. (2008), "Blast response of a lined cavity in a porous saturated soil", *Int. J. Impact. Eng.*, **35**(9), 953-966.
- Feng, S.F., Wang, M.Y., Ren, G.H. and Li, J. (2011), "Research on calculation method for local impact of deep tunnel lining structure", *Chin. J. Rock Mech. Eng.*, **30**(6), 1149-1156.
- Gao, M., Gao, G.Y., Wang, Y. and Feng, S.J. (2010), "Analytical solution on dynamic response of lining subjected to sudden internal uniform loading", *Chin. J. Geotech. Eng.*, **32**(2), 237-242.
- Gu, J.Z. (2015), "Some practical considerations in designing underground station structures for seismic loads", *Struct. Eng. Mech.*, **54**(3), 491-500.
- Guo, S.B., Wang, M.Y., Zhao, Y.T. and Luo, K.S. (2004), "Dynamic numerical analysis of underground structures under action of explosion seismic wave", *World Inform. Earthq. Eng.*, **20**(4), 137-142.
- Jiang, N. and Zhou, C.B. (2012), "Blasting vibration safety criterion for a tunnel liner structure", *Tunnel Underground Space Technol.*, **27**(1), 52-57.
- Lu, Y., Wang, Z. and Chong, K. (2005), "A comparative study of buried structure in soil subjected to blast load using 2D and 3D numerical simulations", *Soil Dyn. Earthq. Eng.*, **25**(4), 275-288.
- Ma, W. (2008), "Investigations of effects of blast vibration and behaviors of impacting failure of underground pipeline structure", *J. PLA Univ. Sci. Technol., Nat. Sci.*, **9**(1), 39-46.
- Mazek, S.A. and Wahab, M.M.A. (2015), "Impact of composite materials on buried structures performance against blast wave", *Struct. Eng. Mech.*, **53**(3), 589-605.
- Nateghi, R., Kiany, M. and Gholipouri, O. (2009), "Control negative effects of blasting waves on concrete of the structures by analyzing of parameters of ground vibration", *Tunnel Underground Space Technol.*, **24**(6), 508-515.
- Olmati, P., Petrini, F. and Bontempi, F. (2013), "Numerical analyses for the structural assessment of steel buildings under explosions", *Struct. Eng. Mech.*, **45**(6), 803-819.
- Penzen, J. and Wu, C.L. (1988), "Stress in linings of bored tunnels", *Earthq. Eng. Struct. Dyn.*, **27**(3), 283-300.
- Shen, J., Gu, J.C., Chen, A.M., Xu, J.M., Ming, Z.Q. and Zhang, X.Y. (2007), "Development and applications of the model test apparatus on anti-explosion structures in geotechnical engineering", *Chin. J. Underground Space Eng.*, **3**(6), 1077-1080.
- Shin, J.H., Moon, H.G. and Chae, S.E. (2011), "Effect of blast induced vibration on existing tunnels in soft rocks", *Tunnel Underground Space Technol.*, **26**(1), 51-61.
- Xin, K., Jiang, X.L. and Wu, X.Y. (2009), "Experimental study on structure response in two-phase saturated soil under blasting load", *Chin. J. Rock Mech. Eng.*, **28**(S1), 4065-4070.